

A Novel Graph Neural Network based Approach for Human Activity Recognition

1st Ritesh Chandra Tewari
ATDC
IIT Kharagpur
Kharagpur, India
rittewari92@gmail.com

2nd Patitapaban Palo
Dept. of Electrical
IIT Kharagpur
Kharagpur, India
patitapabanpalo@gmail.com

3rd Aurobinda Routray
Dept. of Electrical
IIT Kharagpur
Kharagpur, India
aurobinda.routray@gmail.com

4th Jhareswar Maiti
Dept. of Industrial and Systems
IIT Kharagpur
Kharagpur, India
jmaiti@iem.iitkgp.ac.in

Abstract—Human activity recognition (HAR) is an important research area that involves detecting and classifying human activities using various sensors. Recently, radar-based HAR systems have attracted the attention of researchers due to their superiority over other techniques. However, one of the main challenges in HAR is capturing the spatial dependencies among the micro-Doppler features, as the spatial arrangement of the activities and their features are necessary for accurate recognition. This paper introduces a novel graph neural network model for classifying human activities using superpixel gray-scale images constructed from the range and velocity profile obtained from human activity data. Our approach utilizes a k-NN (k-nearest neighbor) graph structure to represent the superpixels as nodes, enabling the model to learn spatial dependencies among the image features. We evaluate the performance of our model with a publicly available dataset using different GNN (Graph Neural Network) techniques, including GCN (Graph Convolution Neural Network), GAT (Graph Attention Network), and SGC (Simplifying Graph Convolution Network), and conduct a comparative study to determine the most effective approach for this task. The results indicate that GAT outperforms the other state-of-the-art techniques in accurately classifying human activities with competitive accuracy.

Index Terms—Human activity recognition, GNN, GCN, SGC, GAT

I. INTRODUCTION

Human activity recognition (HAR) has gained significant research attention due to its versatility and the broad range of potential applications, such as smart homes, healthcare, gaming, fitness tracking, and assisted living [1]–[6]. HAR system aims to categorize human movements into pre-defined activities. Present human activity detection methods can be divided into two categories: wearable and non-wearable. Wearable devices such as accelerometers, push-button devices, and smartphones are more established and widely used [1]. However, it causes discomfort to the users as it has to be attached to the body all the time. Non-wearable devices, on the other hand, include technologies like infrared sensors, microphones, pressure sensors, radar, and cameras. Among non-wearable systems, camera-based systems [2] are the most commonly used, but they face several challenges, including privacy concerns for users. Additionally, occlusion and low lighting conditions can limit their performance. Other types of non-wearable systems, like floor and microphone sensors, are

still largely in the experimental stage and have yet to become viable commercial solutions.

The rise of smart homes has led to increased interest in non-contact indoor monitoring using radar-based technology, as radar signals can penetrate obstacles like walls to detect targets. Furthermore, radar-based methods do not compromise the user's privacy, and there is no need to always wear the sensor. Frequent-modulated continuous wave (FMCW) radars have become popular as active monitoring sensors due to their attractive features like resistance to multi-path fading, better penetration, more precise time resolution, and higher spatial resolution [3].

The underlying principle of a radar-based HAR system is rooted in the concept of Doppler frequency shifts resulting from human activity, which produce corresponding unique signatures [4]. These signatures carry hidden features and are further used for classification using various methods. Traditional machine learning methods [5] depend on manually designed features, which can limit their ability to generalize to new data. Moreover, the process of manually extracting features is both time-consuming and ineffective. On the other hand, deep learning methods take a hierarchical approach to automatically learn high-level features and have demonstrated outstanding results in human activity recognition [6].

Recent advances in machine learning have led to the development of a number of techniques for extracting features from structured graph data. Graph neural networks (GNN) are a fundamental application of deep learning techniques in the graph domain [7]. In [8], the authors present a graph convolutional propagation algorithm for classification at the graph level. Nevertheless, [9] implements the same strategy using a single weight matrix per layer. Spectral graph convolutions are a common way for implementing GCN [10] due to their fast localized convolutions. GCN first learns a first-order spectral filter before layer stacking and activation. GCN has applications in disciplines such as natural language processing [11], citation networks [9], image classifications [12], seismic fault [13] and social networks [14], among others. Further, the authors in [15] present a GNN-based image classification that extracts features from superpixels in a region adjacency graph (RAG).

Our proposed methodology is shown in Fig. 1. First, we derive

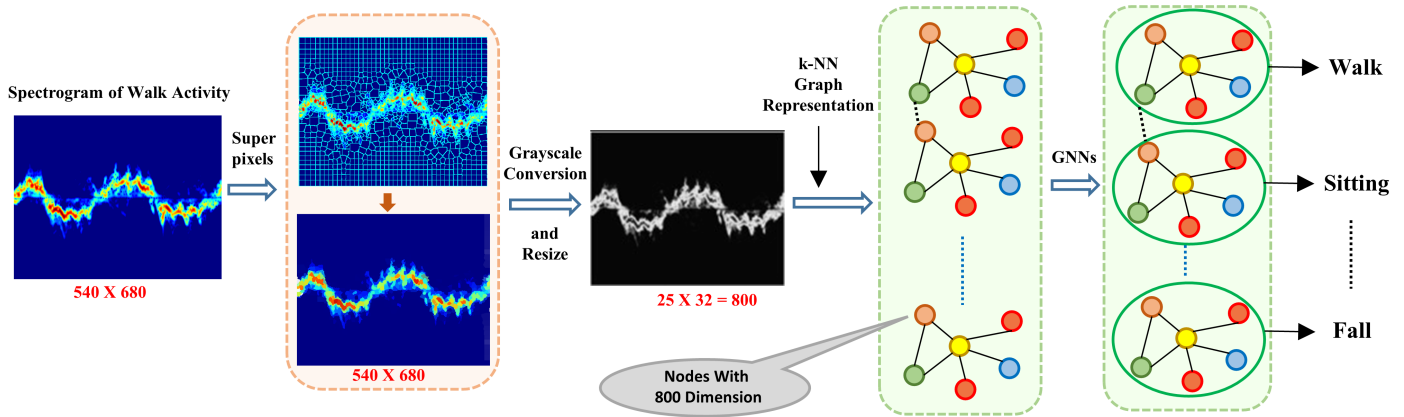


Fig. 1: Proposed Methodology

the range-time (range profile) and velocity-time (spectrogram or velocity profile) plots of radar data associated with the different human activities. Following normalization, we use superpixels for image segmentation, dividing the image into groups of similar pixels in color and texture. Then we convert the superpixel images into grayscale images and use these superpixel matrices as nodes in the graph structure to implement the task as a node classification problem. We use k-NN(k=8, obtained through various experiments using cross-validation) for graph representation and use three different GNN models to compare the results.

Our main contributions to this study are as follows:

- We derive range-time and velocity-time profiles of the sensor data corresponding to different human activities and conduct a comparative study between these profiles to obtain the optimal result.
- We present a novel graph neural network model that leverages the k-nearest neighbor graph structure of superpixel grayscale images derived from the range and velocity profile of radar data to classify various human activities. We evaluate the performance of different GNNs, including GCN, GAT, and SGC, and conduct a comprehensive comparative analysis.

II. DATA PREPARATION

A. Description of Data

We have used a publicly available dataset provided by the University of Glasgow [16]. Data is collected through a 5.8 GHz frequency modulated continuous wave (FMCW) radar with a 400 MHz bandwidth and 1 ms chirp duration. The complex time series of the backscattering signal is collected, where both the amplitude and phase of the signal are affected by the target's electromagnetic features and kinematics. A sample data (d) format is shown below:

$$d = a + ib \quad (1)$$

where a represents the amplitude of the in-phase signal, and b represents the amplitude of the quadrature signal.

Most of the data were collected at the University of Glasgow.

A few parts were obtained from North Glasgow Housing Association facilities, and the Age UK West Cumbria Centre. Participants were encouraged to perform several repetitions of six different activities, which included walking back and forth from the sensor, sitting down on a chair, standing up from a chair, bending forward to pick up an object, drinking from a cup or glass, and performing a frontal fall. All the data were collected in a controlled laboratory environment with physically fit volunteers. The duration of the walking data was 10 seconds, while all other activities had a span of 5 seconds.

B. Preprocessing

All radar-based healthcare systems revolve around three domains of data representation, i.e., range, time, and velocity. Range and velocity are fundamental parameters containing information about human activity [17]. In our work, we considered two data representations, i.e., range-time and velocity-time plots, and compared their feasibility in classifying different activities. These plotted images provide a visual representation of the movements of different body parts, distinguishing between heavier and lighter movements. The oscillations in the images indicate the specific movements, and the resulting signature varies according to the type of movement being performed, thereby indicating the feasibility of utilizing these signatures to uniquely identify human activities.

To obtain these plots, the data is first arranged in a matrix of dimension $m \times n$. Here, m represents the number of time samples per sweep, and n represents the number of chirps. In our case, the data matrix size is 128×5000 ($m = 128$ and $n = 5000$). Fig. 2 shows the steps in finding different plots.

1) *Range-time*: Range information provides the physical distance from the radar to the subject and generally involves the body's macro movements. The range-time plot corresponding to different human activity data provides the subject's distance from the radar position as time varies. A fast Fourier transform (FFT) is applied to each chirp to obtain a range-time plot. This plot can be utilized to classify different human activities. However, we must derive a velocity-time plot for detailed movement information on the limbs.

III. METHODOLOGY

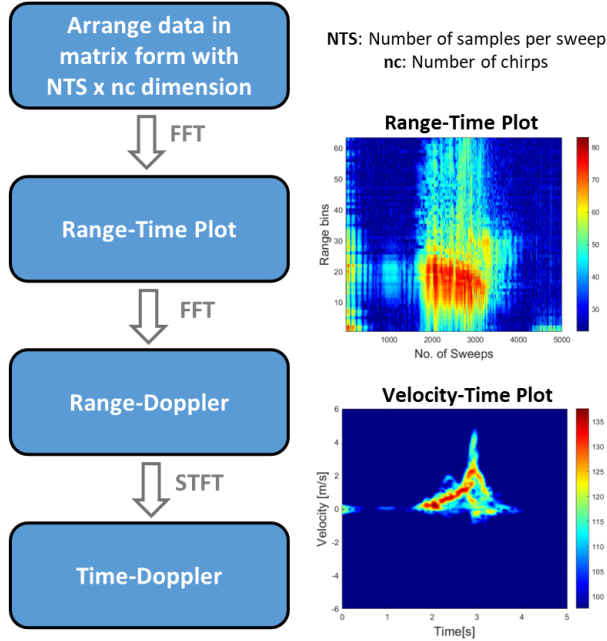


Fig. 2: Steps involved to find range and velocity profile from radar sensor data

2) *Velocity-time*: Unlike range-time, the velocity-time profile gathers information about the body’s micro-movements. During various human activities, it tracks the minute movements of hands, legs, and other limbs. In the range-time matrix, an FFT across the time dimension gives a range-doppler plot. Then, short-time Fourier transform (STFT) is applied with A Hamming window of length 200 with 50% overlap along slow-time for each range bin to generate spectrogram or time-Doppler or velocity-time plots to characterize velocity over time.

3) *Superpixels*: Superpixels are a widely used image segmentation technique that groups similar pixels together based on their color and texture characteristics. Superpixel algorithms aim to generate a compact and meaningful image partition into regions corresponding to objects or object parts. This is achieved by minimizing a cost function that balances the local similarity and the spatial proximity of the pixels. The resulting superpixels can be used as a compact representation of an image for various computer vision tasks, such as object recognition, edge detection, and image compression. By reducing the number of pixels in an image, superpixels can speed up processing time and improve the accuracy of downstream tasks [18]. In our work, superpixels serve as a feature matrix at each graph node.

4) *Grayscale Conversion*: We convert the obtained superpixel images into grayscale images for further processing. Grayscale images have lower dimensionality, making them computationally less expensive to process than color images. This is particularly important in GNNs, where the computational complexity increases with the number of features.

In graphs, data elements are connected based on certain relationships. The graph is expressed as $\mathcal{G} = (\mathcal{V}, \mathcal{E})$, where \mathcal{V} is a set of N vertices or nodes, represented by $\{\mathcal{V}_0, \mathcal{V}_1, \dots, \mathcal{V}_{N-1}\}$, and \mathcal{E} is the set of edges connecting the nodes. The relationship between nodes is represented by an $N \times N$ adjacency matrix, where the weight of the edge connecting node i and j , denoted as $\mathcal{E}_{i,j} \in \mathcal{C}$, where \mathcal{C} is a set of complex numbers. The set of nodes connected to vertex \mathcal{V}_n is referred to as the neighborhood, $W_n = \{j | \mathcal{E}_{i,j} \neq 0\}$.

In this method, a graph of nearest neighbors is utilized. The graph $\mathcal{G} = (\mathcal{V}, \mathcal{E})$ consists of N vertices, representing N different superpixels of plot images. Each image of size $m \times n$ is considered a point in an $m * n$ dimensional vector space. To determine the graph, the Euclidean distance between all superpixels is calculated, and a k-nearest neighbor graph is constructed, with k set to eight for optimal computation time and accuracy across six data classes. The Euclidean distance is computed based on the superpixel values in the $m * n$ -dimensional vector space. The corresponding vertices are connected if two superpixels of images belong to the same class and the superpixel values are among the eight nearest elements. The graph can also be represented as a weighted graph by assigning weights to the edges $\mathcal{E}_{i,j} = \exp(\delta_{i,j}^2)$, where $\delta_{i,j}$ is the Euclidean distance between the i^{th} and j^{th} vertices. In an unweighted graph, the weight is set to one if two vertices are connected and zero otherwise. In this study, we apply three different graph neural network models, which are graph convolution network (GCN), graph attention network (GAT), and simple graph convolution (SGC).

1) *GCN*: The GCN model employs a localized approximation of spectral graph convolutions to construct the convolutional architecture, as described by Kipf et al. [9]. GCNs are typically designed as semi-supervised models with multiple layers. The output of a GCN with two layers can be mathematically expressed as:

$$O = f(\mathcal{F}, \mathcal{E}) = \text{ReLU}(\hat{\mathcal{E}} \text{ReLU}(\hat{\mathcal{E}} \mathcal{F} \omega^{(0)})) \omega^{(1)} \quad (2)$$

where, $\hat{\mathcal{E}} = \tilde{\mathcal{D}}^{-1/2} \tilde{\mathcal{E}} \tilde{\mathcal{D}}$, $\tilde{\mathcal{D}}_{ii} = \sum_j \tilde{\mathcal{E}}_{i,j}$, is the degree matrix. $\tilde{\mathcal{E}} = \mathcal{E} + I_{|\mathcal{V}|}$, where \mathcal{E} is the original adjacency matrix and $I_{|\mathcal{V}|}$ is the identity matrix and $\omega^{(0)}$ and $\omega^{(1)}$ are the weight matrices.

2) *GAT*: The GAT model, unlike GCN, directly utilizes the spatial information of each node in the graph to learn the representation of each node. GAT achieves this by using node self-attention and neighboring features to train the model, similar to GCN [19]. The attention coefficient is determined by performing self-attention using a weight matrix ω and input features \vec{f}_i .

$$c_{i,j} = e(\omega \vec{f}_i, \omega \vec{f}_j) \quad (3)$$

The masked attention is performed by computing $c_{i,j}$ for nodes $j \in W$ and then normalizing by applying the softmax function to the computed attentions. The aggregation is carried

out using multi-head attention averaging rather than a scalar attention score, which is expressed as:

$$\vec{f}_i = \sigma \left(\frac{1}{N} \sum_{k=1}^N \sum_{j \in W_i} e_{i,j}^k \omega^k \vec{f}_j \right) \quad (4)$$

Here, ω^k is the weight matrix for the k^{th} attention head, and $e_{i,j}^k$ is the attention coefficient for the i^{th} node and the j^{th} neighboring node. The activation function σ is applied element-wise to the aggregated result.

3) *SGC*: The SGC model is a simplified version of the GCN model. In SGC, non-linearities are removed sequentially, and weight matrices between subsequent layers are compressed. The model involves a graph-based preprocessing phase followed by a standard multi-class logistic regression for classification [20]. The SGC classification formulation can be expressed as follows:

$$O = \text{softmax}(\hat{E}^N F \omega) \quad (5)$$

Here, ω is the weight matrix, and N is the number of layers.

IV. RESULTS AND DISCUSSION

In this study, we considered two different radar data representations, range profile and velocity profile, as inputs to our proposed models after proper preprocessing (II-B). To determine the optimal outcome, we varied the superpixel values and image sizes for comparison purposes. We investigated the effect of varying superpixel values (fixing the image size to 25×32) on the classification accuracy of three distinct methods: GCN, SGC, and GPT. We ran each model for 40 epochs, except for GAT, which we ran for 1000 epochs (as the standard set by respective literatures [9], [19], [20]). We repeated the experiment 100 times for each model to calculate the average accuracy. Table I shows the obtained results. We also plotted the variation of average accuracy with changing superpixel values, as shown in Fig. 3 and 4. Our findings indicate that GAT performed best with 1000 superpixels, obtaining an accuracy of 97.81% for the velocity profile. For the range profile, we achieved 95.70% accuracy with 300 superpixels, clearly depicting the superiority of the spectrogram in representing human activity. In addition, we compared the results obtained for different image sizes (using a specific superpixel value of 600). The comparison outcome is presented in Table II. Surprisingly, increasing the image size did not result in a higher accuracy rate. Thus, we recommend using a superpixel value of 1000 and an image size of 25×32 for the best results with the velocity profile.

To evaluate the performance of our proposed method, we compared it with current state-of-the-art methods in the literature. As shown in Table III, our proposed GAT method achieved the highest accuracy of 97.81%, outperforming all other methods. The other methods in the table range from 89.50% to 97.58% in accuracy, further highlighting our proposed method's superior performance. The key advantage of our proposed GAT method is its ability to effectively capture the spatial dependencies among the features extracted from

sensor data. It uses a graph-based approach, which models the relationship between the features as a graph and uses attention mechanisms to weigh the importance of different nodes in the graph, enabling the model to effectively learn the complex patterns in the sensor data and achieve high accuracy in human activity recognition.

TABLE I: Comparison of Different Superpixels

Super Pixel	Velocity Profile			Range Profile		
	GCN	SGC	GAT	GCN	SGC	GAT
100	53.92	88.33	90.32	72.25	87.79	89.61
200	51.5	87.95	88.33	73.38	88.33	92.47
300	72.04	91.88	90.32	64.67	90.32	95.70
400	69.89	91.93	92.47	71.88	90.00	92.47
500	73.22	90.64	90.86	72.63	88.38	89.74
600	80.53	91.18	94.09	66.20	90.32	92.47
700	80.16	90.86	90.32	70.00	91.18	93.55
800	75.59	89.99	94.09	67.74	89.57	94.62
900	58.06	90.10	93.55	75.37	90.48	95.16
1000	55.86	90.10	97.81	73.38	90.8	94.09
1100	92.85	90.21	92.47	68.17	91.39	94.09
1200	63.81	90.91	92.47	74.83	92.36	94.09
1300	56.02	90.96	92.47	68.28	91.66	93.55
1400	71.02	90.80	91.94	68.22	90.00	93.01
1500	64.73	91.13	94.62	77.09	91.02	94.62
1600	63.06	89.83	91.40	67.90	90.00	93.01

Image Size = 25×32

TABLE II: Comparison of Different Image Size

Image Size	Velocity Profile			Range Profile		
	GCN	SGC	GAT	GCN	SGC	GAT
25×32	80.53	91.18	94.09	66.20	90.32	92.47
54×64	51.82	90.59	86.33	46.95	84.87	83.32
75×96	71.29	91.98	82.51	42.16	85.38	77.91
100×128	15.59	91.2	15.59	15.59	80.64	15.59

Superpixels = 600

TABLE III: Comparison With Previous Works

Reference	Method Used	Accuracy
[21]	CNN	91%
[6]	bi-LSTM	95.90%
[22]	Sensor Fusion	91.30%
[23]	SVM+ANN	96%
[5]	SVM (cubic kernel)	94%
[24]	RD-CNN	89.50%
[25]	T-CNN	97.58%
[26]	RNN	94.30%
[27]	VGG-Net	95.80%
[28]	DCGAN+CNN	97.20%
Proposed	GAT	97.81%

ANN = Artificial neural network, SVM = Support Vector Machine, RD-CNN = Range-Distributed Convolution Neural Network, T-CNN = Tower Convolution Neural Network, RNN = Recurrent Neural Network, CNN = Convolution Neural Network, DCNN = Deep Convolution Neural Network, Bi-LSTM = Bidirectional Long Short Term Memory, DCGAN = Deep Convolutional Generative Adversarial Network, VGG-Net = Visual Geometry Group Network

V. CONCLUSION AND FUTURE SCOPE

The present study explores the potential of graph neural networks (GNNs) for radar-based human activity recognition

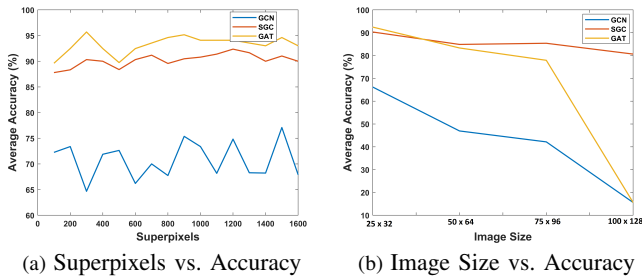


Fig. 3: Accuracy dependency on superpixels and image size of the range profile of the radar human activity data.

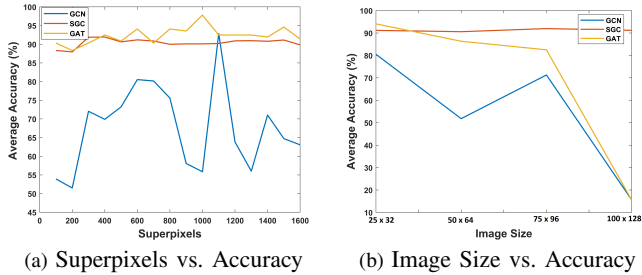


Fig. 4: Accuracy dependency on superpixels and image size of the velocity profile of the radar human activity data.

(HAR). Different GNN models and the current state-of-the-art approach were compared to evaluate their performance. GNN models, specifically GAT, showed a significant increase in classification accuracy. We considered two distinct radar data representations to demonstrate the potential of GNNs for human activity detection. As part of future work, we will evaluate the performance of GNNs in the presence of noise. This evaluation will enable us to understand better the ability of GNNs to handle noisy inputs and identify potential limitations of the current model in such scenarios.

REFERENCES

- [1] A. Bulling, U. Blanke, and B. Schiele, "A tutorial on human activity recognition using body-worn inertial sensors," *ACM Computing Surveys (CSUR)*, vol. 46, no. 3, pp. 1–33, 2014.
- [2] J. Qin, L. Liu, Z. Zhang, Y. Wang, and L. Shao, "Compressive sequential learning for action similarity labeling," *IEEE Transactions on Image Processing*, vol. 25, no. 2, pp. 756–769, 2016.
- [3] N. F. M. Ariffin, F. N. M. Isa, and A. F. Ismail, "Fmcw radar for slow moving target detection: Design and performance analysis," in *2016 International Conference on Computer and Communication Engineering (ICCCCE)*, 2016, pp. 396–399.
- [4] Y. Lin, J. Le Kerneç, S. Yang, F. Fioranelli, O. Romain, and Z. Zhao, "Human activity classification with radar: Optimization and noise robustness with iterative convolutional neural networks followed with random forests," *IEEE Sensors Journal*, vol. 18, no. 23, pp. 9669–9681, 2018.
- [5] A. Shrestha, J. Le Kerneç, F. Fioranelli, E. Cippitelli, E. Gambi, and S. Spinsante, "Feature diversity for fall detection and human indoor activities classification using radar systems," in *International Conference on Radar Systems (Radar 2017)*, 2017, pp. 1–6.
- [6] H. Li, A. Shrestha, H. Heidari, J. Le Kerneç, and F. Fioranelli, "Bi-lstm network for multimodal continuous human activity recognition and fall detection," *IEEE Sensors Journal*, vol. 20, no. 3, pp. 1191–1201, 2020.
- [7] Z. et. al., "A comprehensive survey on graph neural networks," *IEEE Transactions on Neural Networks and Learning Systems*, vol. 32, no. 1, pp. 4–24, 2021.

- [8] M. Defferrard, X. Bresson, and P. Vandergheynst, "Convolutional neural networks on graphs with fast localized spectral filtering," in *Proceedings of the 30th International Conference on Neural Information Processing Systems*, ser. NIPS'16. Curran Associates Inc., 2016, p. 3844–3852.
- [9] T. N. Kipf and M. Welling, "Semi-supervised classification with graph convolutional networks," *arXiv preprint arXiv:1609.02907*, 2016.
- [10] D. et. al., "Convolutional networks on graphs for learning molecular fingerprints," in *Advances in Neural Information Processing Systems*, vol. 28. Curran Associates, Inc., 2015, pp. 2224–2232.
- [11] L. Yao, C. Mao, and Y. Luo, "Graph convolutional networks for text classification," *Proceedings of the AAAI Conference on Artificial Intelligence*, vol. 33, no. 01, pp. 7370–7377, Jul. 2019.
- [12] B. Knyazev, X. Lin, M. R. Amer, and G. W. Taylor, "Image classification with hierarchical multigraph networks," *CoRR*, vol. abs/1907.09000, 2019.
- [13] P. Palo, A. Routray, R. Mahadik, and S. Singh, "Fault detection in seismic data using graph convolutional network," *The Journal of Supercomputing*, pp. 1–29, 2023.
- [14] S. Abu-El-Haija, A. Kapoor, B. Perozzi, and J. Lee, "N-GCN: multi-scale graph convolution for semi-supervised node classification," *CoRR*, vol. abs/1802.08888, 2018.
- [15] P. H. C. Avelar, A. R. Tavares, T. L. T. da Silveira, C. R. Jung, and L. C. Lamb, "Superpixel image classification with graph attention networks," *CoRR*, vol. abs/2002.05544, 2020.
- [16] F. Fioranelli, S. A. Shah, H. Li, A. Shrestha, S. Yang, and J. Le Kerneç, "Radar signatures of human activities," 2019.
- [17] D. F. Fioranelli, D. S. A. Shah, H. Li, A. Shrestha, D. S. Yang, and D. J. L. Kerneç, "Radar sensing for healthcare: Associate editor francesco fioranelli on the applications of radar in monitoring vital signs and recognising human activity patterns," *Electronics Letters*, vol. 55, no. 19, pp. 1022–1024, 2019.
- [18] R. Achanta, A. Shaji, K. Smith, A. Lucchi, P. Fua, and S. Süsstrunk, "Slic superpixels compared to state-of-the-art superpixel methods," *IEEE Transactions on Pattern Analysis and Machine Intelligence*, vol. 34, no. 11, pp. 2274–2282, 2012.
- [19] P. Veličković, G. Cucurull, A. Casanova, A. Romero, P. Lio, and Y. Bengio, "Graph attention networks," *arXiv preprint arXiv:1710.10903*, 2017.
- [20] F. Wu, A. Souza, T. Zhang, C. Fifty, T. Yu, and K. Weinberger, "Simplifying graph convolutional networks," in *International conference on machine learning*. PMLR, 2019, pp. 6861–6871.
- [21] S. Li, M. Jia, J. L. Kerneç, S. Yang, F. Fioranelli, and O. Romain, "Elderly care: Using deep learning for multi-domain activity classification," in *2020 International Conference on UK-China Emerging Technologies (UCET)*, 2020, pp. 1–4.
- [22] H. Li, A. Shrestha, F. Fioranelli, J. Le Kerneç, H. Heidari, M. Pepa, E. Cippitelli, E. Gambi, and S. Spinsante, "Multisensor data fusion for human activities classification and fall detection," in *2017 IEEE SENSORS*, 2017, pp. 1–3.
- [23] H. Li, A. Shrestha, H. Heidari, J. Le Kerneç, and F. Fioranelli, "Magnetic and radar sensing for multimodal remote health monitoring," *IEEE Sensors Journal*, vol. 19, no. 20, pp. 8979–8989, 2019.
- [24] W.-Y. Kim and D.-H. Seo, "Radar-based human activity recognition combining range-time-doppler maps and range-distributed-convolutional neural networks," *IEEE Transactions on Geoscience and Remote Sensing*, vol. 60, pp. 1–11, 2022.
- [25] A. Helen Victoria and G. Maragatham, "Activity recognition of fmcw radar human signatures using tower convolutional neural networks," *Wireless Networks*, pp. 1–17, 2021.
- [26] H. Jiang, F. Fioranelli, S. Yang, O. Romain, and J. Le Kerneç, "Human activity classification using radar signal and rnn networks," in *IET International Radar Conference (IET IRC 2020)*, vol. 2020, 2020, pp. 1595–1599.
- [27] F. A. Jibrin, A. Abdulaziz, A. S. Muhammad, A. Usman, and Y. Jibril, "Indoor human activity classification based on fmcw radar micro-doppler signatures and deep-learning networks," in *2021 1st International Conference on Multidisciplinary Engineering and Applied Science (ICMEAS)*, 2021, pp. 1–5.
- [28] R. C. Tewari, P. Palo, J. Maiti, and A. Routray, "Gan-based radar micro-doppler augmentation for high accuracy fall detection system," in *IECON 2022 – 48th Annual Conference of the IEEE Industrial Electronics Society*, 2022, pp. 1–6.